



Analysis of COSIMA spectra: Bayesian approach

H. J. Lehto¹, B. Zaprudin¹, K. M. Lehto², T. Lönnberg³, J. Silén⁴, J. Rynö⁴,
H. Krüger⁵, M. Hilchenbach⁵, and J. Kissel⁵

¹Tuorla Observatory, Department of Physics and Astronomy, University of Turku,
Väisäläntie 20, 21500 Piikkiö, Finland

²Molecular Plant Biology, Department of Biochemistry, University of Turku,
20014 Turku, Finland

³Organic Chemistry, Department of Chemistry, University of Turku,
20014 Turku, Finland

⁴Finnish Meteorological Institute, Erik Palmenin aukio 1, PB 503, 00101 Helsinki, Finland

⁵Max Planck Institute for Solar System Research Justus-von-Liebig-Weg 3,
37077 Göttingen, Germany

Received: 16 June 2014 – Accepted: 8 October 2014 – Published: 11 November 2014

Correspondence to: H. J. Lehto (hlehto@utu.fi)

Published by Copernicus Publications on behalf of the European Geosciences Union.

Title Page

Abstract

Introduction

Conclusions

References

Tables

Figures

◀

▶

◀

▶

Back

Close

Full Screen / Esc

Printer-friendly Version

Interactive Discussion



Abstract

We describe the use of Bayesian analysis methods applied to TOF-SIMS spectra. The method finds the probability density functions of measured line parameters (number of lines, and their widths, peak amplitudes, integrated amplitudes, positions) in mass intervals over the whole spectrum. We discuss the results we can expect from this analysis. We discuss the effects the instrument dead time causes in the COSIMA TOF SIMS. We address this issue in a new way. The derived line parameters can be used to further calibrate the mass scaling of TOF-SIMS and to feed the results into other analysis methods such as multivariate analyses of spectra. We intend to use the method in two ways, first as a comprehensive tool to perform quantitative analysis of spectra, and second as a fast tool for studying interesting targets for obtaining additional TOF-SIMS measurements of the sample, a property unique for COSIMA. Finally, we point out that the Bayesian method can be thought as a means to solve inverse problems but with forward calculations only.

1 Introduction

The COmetary Secondary Ion Mass Analyzer (COSIMA) is a time-of-flight secondary ion mass spectrometer (TOF-SIMS) on board the Horizon 2000 European Space Agency Rosetta mission en route to encounter the comet 67P/Churyumov–Gerasimenko. The space probe consists of an orbiter and a lander. After the in-flight hibernation, the space probe and its instruments were successfully woken up on 20 January 2014. The first orbital maneuvers for the comet approach took place in May 2014. The formal mission end date is 31 December 2015. By that date the comet has passed perihelion with the Rosetta spacecraft clinging near it all the time. While the orbiter is traveling at slow speed (meters per second) in the vicinity of the comet (Glassmeier et al., 2007), the COSIMA instrument is collecting dust particles that have been expelled by the comet. A representative set of these particles enter into

Title Page

Abstract

Introduction

Conclusions

References

Tables

Figures

◀

▶

◀

▶

Back

Close

Full Screen / Esc

Printer-friendly Version

Interactive Discussion



COSIMA: Bayesian analysis

H. J. Lehto et al.

Title Page

Abstract

Introduction

Conclusions

References

Tables

Figures

I◀

▶I

◀

▶

Back

Close

Full Screen / Esc

Printer-friendly Version

Interactive Discussion



COSIMA through an open window which extends to the outer surface of Rosetta. The particles are collected on a target plate, which consists of three square 1 cm by 1 cm metal plates and an unexposed 0.3 by 3.0 cm reference area. Once exposed the plate is stored. At a suitable time the plates are examined one by one with an illuminated optical microscope, the COSISCOPE which has an optical pixel size resolution of 14 μm (Kissel et al., 2007). By combining several exposures a super resolution of about 3 μm is possible. Target particles for further analysis are selected, and exposed to an ^{115}In primary ion beam with an ion energy of +8 KeV, a pulse duration of < 3 ns, and a beam width of 50 μm . During each pulse an unknown number of secondary ions are expelled from the top layer(s) of the target sample created. These secondary ions then enter the electric field lens system and end up on the detector, where the flight times of ions are measured. For short this process is called a shot. Depending on the polarity, positive or negative ions are detected. The shots are repeated at 500 μs intervals, thus a one second exposure consists of 2000 shots and during a 3 min exposure about 360 000 shots are fired. The instrument is described in detail by Kissel et al. (2007).

The outcome of a measurement is a time of flight spectrum, which we are directly interested in. In this paper we will discuss the quantitative foundation of understanding the spectrum through statistical analyses of individual spectral lines and touch on some critical issues such as instrument dead time effects, normalization, isotope ratio calculation of lines. Multivariate techniques connecting complex chemistry and complete spectra are discussed elsewhere (Silén et al., 2014). Bayesian methods can be extended to the interpretation of these cases too, but this is beyond our scope here.

2 Time of flight spectrum

We measure the raw time of flight spectrum, the number of secondary ions as a function of time. This is the coordinate space we are working in.

The time of flight of an ion scale with the mass m and charge q is

$$t = a + b\sqrt{(m/q)}, \quad (1)$$

where a and b have values of about 4000 and 1600, respectively in COSIMA. The values of a and b are initially estimated by the onboard software. The charge q is usually $+1$ or -1 . The mass of the ion m is in atomic mass units, u . The time of flight is digitized by the Time-to-digital converter to bins of 1.953125 ns (Kissel et al., 2007). One COSIMA time of flight time bin t corresponds at mass $m \sim 1$ to $0.0013 u$ and at $m \sim 900$ to about $0.04 u$.

The resolution of the mass spectrometer is $m/\delta m \sim 1400$ at $m = 100$. At low masses all the atomic lines are easily separated. Up to mass off about $m \sim 120 u$ mineral and hydrogen rich organic components can be separated (F. Krüger, personal communication, 1992). The distinction is based on the fact that most minerals due to their internal structure shows elemental masses. These have values that usually are below the integer value of the mass. Single mineral ions with $Z > 80$, $m > 200$ have masses below integer values, but they are not expected to have a large contribution to the spectrum. Hydrogen tends to be common in organic molecules and their breakup products. A neutral hydrogen has a mass surplus of $\delta H = 0.0078 u$ above the integer value of 1. A loss of an electron produces a hydrogen ion, H^+ with an excess of $\delta H^+ = 0.0073 u$. This implies that organic molecules with ample hydrogen tend to have masses above an integer mass value. It is noteworthy to mention that other elements common in organics have the following deviations ^{12}C : $0 \delta H$, ^{14}N : $0.39 \delta H$, ^{16}O : $-0.65 \delta H$, so nitrogen enhances the positive deviation, while the presence of oxygen reduces it. Two relatively common elements, phosphorus and sulfur, often associated with organics reduce the organic shift by ^{31}P : $-3.36 \delta H$, ^{32}S : $-3.56 \delta H$.

The full spectrum consists of 2^{17} or 131 072 time bins and reach to about $m \sim 6400 u$. The raw data is in the form of counts per TOF time bin. The lowest mass peak is usually hydrogen ion at $1.0073 u$. An electron peak at mass $m_e = (1/1839) u$ is present in negative spectra. It is broad due to the significantly larger thermal velocities electrons have



compared to ions and due to the high energy the ion formation and decay processes after the substrate has been irradiated with the indium beam. In principle ions with the same mass should fall into one time bin. However the stability of the instrument, the pulse length of the primary beam, finite beam size and thermal distribution of ions all contribute to the resolution so that the time of flight arrivals from a single pulse produces a peak with a full width at half of the maximum amplitude (FWHM) of about 2.5 TOF time bins, and close to Gaussian in shape.

Dead time effects

The secondary ions have a distribution in arrival times, which can be characterized by a distribution at time of flight corresponding to the true mass and Gaussian dispersion of about 2.5 bins FWHM. In weak lines with low secondary ion yield, most of the firings will produce no secondary ions for that mass, and only single ions will be recorder occasionally. For example a line with a total count of ~ 1000 secondary ions in a 3 min exposure will behave in this way, with about one secondary ion on average for every 360 indium shots.

If the ion yield is higher, such that the total counts of a spectral line are of the order of 10 % of the total number of shots, in our example $\sim 10^4$, then an instrument dead time effect sets in. After the arrival of a secondary ion, the instrument does not respond to new secondary ions within the next 10 ns, which corresponds to about 5.2 TOF time bins (Kissel et al., 2007). This becomes important when the number of cases with two or more ions arriving to the instrument becomes significant. Note also as the instrument cannot distinguish between background ions and “good” ions. Both will contribute to the dead time effect. The contribution of the background is expected to be small, because of the low background levels in COSIMA. It cannot be completely ignored however. The dead time causes two major distortions to the shape of the spectral line. It reduces the total number of counts detected per time of flight bin. Further, a second bias is produced by the asymmetric nature of the dead time. The spectral line becomes

GID

4, 563–588, 2014

COSIMA: Bayesian analysis

H. J. Lehto et al.

Title Page

Abstract

Introduction

Conclusions

References

Tables

Figures

◀

▶

◀

▶

Back

Close

Full Screen / Esc

Printer-friendly Version

Interactive Discussion



skewed by the shifting the peak of the line to smaller flight times than if all ions were recorded or if the dead time was zero.

The single most important parameter for understanding the dead time effect is the ratio of counts creating a given line to the number of shots. It gives a measure of how many occurrences of two or more ions in a single shot occur for that particular line. This implies that two spectra with same line counts for a given mass will have different dead-time effects if they have a different number of shots. On the other hand the shape of the same line in a sample from short exposures and long exposures will not change due to dead time effects if the secondary ion yield does not change.

Ideally the time of flight spectrum would show no background, show sharp discrete line peaks and have an exact TOF mass calibration. In reality we are limited by measurement statistics, finite resolution, dead time effects, background, multiple nearby by lines and various other issues. We will next address how to analyze our COSIMA spectra from a Bayesian perspective.

3 Method (mathematics and statistics)

We discuss next the statistical nature of the data. The ordinate in the data is the TOF time bin, which has a linear relation to the time of flight, which scales as the square root of ion mass. The data itself is count data and thus Poisson distributed.

The parameters we are interested in at a given mass are the number of spectral components, the integrated count of each component, the mass corresponding to each line and the confidence limits of all these parameters. We approximate the spectral lines as Gaussian in the time of flight coordinate system. We will later apply other options such as a combination of a Gaussian and a Lorentzian profile. Standard methods such as least squares or χ^2 fittings are not applicable, however. The reason for this is the nature of the noise in these spectra.

Title Page

Abstract

Introduction

Conclusions

References

Tables

Figures

◀

▶

◀

▶

Back

Close

Full Screen / Esc

Printer-friendly Version

Interactive Discussion



Our data is particle count data and as such positive definite. It follows Poisson statistics. The Poisson probability density function is defined as

$$p(n, \lambda) = \frac{\lambda^n e^{-\lambda}}{n!}, \quad (2)$$

where for large values of n the factorial is calculated either in a logarithmic form

$$\ln(p(n, \lambda)) = n \ln \lambda - \lambda - \ln(n!) \quad (3)$$

or e.g. by the Batir (2010) equation which is good for $n > 1$ to within a relative accuracy of $< 10^{-6}$ which is sufficient for our calculations.

The Poisson nature of the data implies that the distribution is not symmetric. The mean has a value different from the median and the mode, the most likely value. As the distribution is not symmetric, the standard “sigma”, should not be used to calculate confidence limits or “error limits”. Note also that strong peaks have the largest noise in the absolute terms, whereas low peaks have relatively a more significant noise contribution.

The instrumental dead time brings an additional special complication. The observed data which is affected by the dead time still has a Poisson probability distribution in secondary ion counts per time bin. The “correction” of the dead time applied effectively distorts the statistical properties of the data by increasing the real noise in the corrected data to a level larger than what is expected from Poisson data, the corrected data been essentially too noisy. This is potential problem for strong lines. Our approach will avoid these problems.

In statistical analyses, one tends to habitually assume Gaussian noise and the propagation of errors through addition of variances. These assumptions are not valid in our case. Their use could cause negative values in “error” limits, which is mathematically and physically an impossible situation as they would imply negative counts. Furthermore, the way propagation is used contains the hidden assumption of symmetric errors, which is not the case in these data.

We will address the analysis of COSIMA spectra through Bayesian analysis, which will avoid all the problems mentioned above.

3.1 Bayesian analysis

The Bayesian analysis is a universal means of understanding and interpreting measured data. In principle we could consider our spectrum as one measured entity with several hundred lines and interpret the full spectrum by Bayesian means. This would require working in a data space of a dimensionality of several thousands squared. In practice it is more convenient to reduce the analysis into analysis of hundreds of lines, which can be really a combination of several nearby lines. This we can do as at low masses there is no overlap between lines of different integer masses and at high masses the lines tend to be sparse and still well separated.

Assume that you have an observed peak shape $Y_0(t)$, where t represents a time bin. It is a sum of the true unknown peak shape $\theta(t)$ and a noise term $n_0(t)$. If we have prior knowledge of a likely beam shape we may assume this shape. It does not mean that we fix the beam shape for good, as we can later apply other models and compare them objectively. This is one of the benefits of Bayesian analysis. It is however good to have a reasonable starting model. The simplest model is that there is no signal in the data and that at an mass interval the $y(t)$ is constant. Using a single Gaussian added to a constant background will require 3 additional parameters, the amplitude, the width and the center of line and for each additional Gaussian we need three more parameters. In our model we need further to take into account the dead-time effects which affect several bins at a time. Our model is thus of the form

$$\theta(t) = D(y(t, x_n)), \quad (4)$$

here $\theta(t)$ is the calculated model, $D(\cdot)$ is dead time effect, y is the model which is a function of time, and n is the number of parameters, one for background and three additional parameters for each Gaussian.

GID

4, 563–588, 2014

COSIMA: Bayesian analysis

H. J. Lehto et al.

Title Page

Abstract

Introduction

Conclusions

References

Tables

Figures

◀

▶

◀

▶

Back

Close

Full Screen / Esc

Printer-friendly Version

Interactive Discussion



COSIMA: Bayesian analysis

H. J. Lehto et al.

Title Page

Abstract

Introduction

Conclusions

References

Tables

Figures

I◀

▶I

◀

▶

Back

Close

Full Screen / Esc

Printer-friendly Version

Interactive Discussion



We will search for a solution from the values of model parameters $\theta = \theta(i, x_n)$ that best describes the observed spectrum $Y_0(i)$, note the time is discrete, we use now i instead of the t for continuous time. To within a normalization constant we can directly calculate for each point t the probability p that our observed data $Y(i)$ is explained by a given model θ . Multiplying all these individually calculated probabilities we get the conditional probability of our data given the model $p(Y|\theta)$. Note that this is a point where we differ e.g. from a χ^2 minimization as we do not square deviations but rather calculate probabilities. We next take into account any prior information we have of the parameters and their distributions. This probability independent of the data is called the prior probability density $p(\theta)$. It can be considered as the sampling probability space of the data in the parameters space of the model. By multiplying these two probability densities we get the probability distribution of the the values of θ that explain our data.

Mathematically we are interested in knowing what is the best model θ that describes our data.

$$p(\theta|Y) \propto p(\theta)p(Y|\theta) \quad (5)$$

The posteriori density $p(\theta|Y)$ describing the probability density function of the model parameters is thus proportional to the product of the prior density of the model parameters $p(\theta)$ and the probability of the sampling distribution, the data based on the model $p(Y|\theta)$. This is a simplified version of the Bayesian inference (Gelman et al., 1995).

The prior densities $p(\theta)$ are selected such that the position has a uniform density in a mass interval $(m - 0.5, m + 0.5]$: the amplitude of the peak is not well determined in advance, so we have given a prior distribution which is non-informative, i.e. flat in $10 \log(\text{amplitude} + 1)$. The prior density for the peak width is somewhat cumbersome. We know that the value cannot be negative, and not likely to be very wide. The FWHM of the peak of the COSIMA is expected to be close to about 2.5 or a sigma of 1.1 TOF time bins. To take this into account we apply a prior density distribution $\propto (\lg(\text{FWHM}/2.5))^{-2}$ Note that this does not rule our solutions with single wide peaks.

It biases also against identifying single high bins as very unrealistic narrow peaks and against modeling a constant background as an extremely wide Gaussian.

Our result, will provide the probability density distribution of various parameters on the left of the equation above. By finding the mode of this distribution we get the most likely value in the model parameter space describing the data. Confidence limits to the model parameters can be calculated from the posteriori probability distributions.

3.2 MCMC algorithms

Markov Chain Monte Carlo chains (MCMC) are very useful in determining the posteriori probability space. A random walk in the parameter space is created. This chain converges to the target distribution which multiplied by the priori distributions will give the posteriori distribution. In creating the random walk sequence the next draw from the parameter space depends on the position and the value of the previous sample.

One widely used family of MCMC chains is the Metropolis algorithm. The core in these algorithms is the decision of whether to accept the next move. Say, that one has calculated the probability $p(\theta_i|Y)$, we make a move from θ_i to θ_{i+1} by selecting randomly a point from the jumping distributions, which have to be symmetric. If the new θ_{i+1} has a higher probability $p(\theta_{i+1}|y)$, then we accept the move. If the probability is poorer it will be accepted if the ratio $p(\theta_{i+1}|y)/p(\theta_i|y) > a$, where a is a random number drawn from a uniform distribution $[0,1)$. The selection of points of lower likelihood allows for an effective sampling of the posteriori distribution. This central part of the decision is shared by many Markov chain algorithms that carry different kinds of names.

We use the adaptive Metropolis algorithm (Haario et al., 2001). It has the same Metropolis jumping criterion as above, but it has different means for selecting an optimized step size and the jumping direction in the d -dimensional parameter space. This is done by means of the covariance matrix of the model parameters. The matrix is calculated from the ever refining posterior distribution in the parameter space. The step size is obtained from the Cholesky decomposition of the variance matrix multiplied by a normalization factor $s_d = 2.4^2/d$, where d is the dimension of the free parameters.

Title Page

Abstract

Introduction

Conclusions

References

Tables

Figures

◀

▶

◀

▶

Back

Close

Full Screen / Esc

Printer-friendly Version

Interactive Discussion



$$\mathbf{X}_k = \mathbf{X}_{k-1} + \sqrt{s_d} \text{Chol}(\mathbf{C}_k) \mathbf{G}, \quad (6)$$

here \mathbf{X}_k is the parameter vector at step k , \mathbf{G} is a random vector from a Normal distribution $\mathbf{N}(0, 1)$ and \mathbf{C}_k is the covariance matrix of the model parameters calculated from a suitable points, and d is the number of parameters in the model (Tamminen, 1994).

For simulated and real spectra we have used typically 200 iterations in the burn in phase and 20 000 in the main iteration phase. The upper limit of iterations is determined by convergence to the posteriori distribution and the confidence levels needed.

4 Calculations

4.1 Effects of the dead time

We performed simulations to measure the effects of dead time in COSIMA. First, to obtain a good handle on the effect of dead time and second to verify that the equations we use in applying the dead time effect are suitable for our Bayesian simulations.

We assume a dead time of 10 ns with a total blockage between the first ion and the subsequent ions. After this dead time, a new ion can be measured initiating a new dead time. From different total secondary ion counts and indium shots we calculate the probability of various numbers of shots from this line. We simulate each shot separately. The number of secondary ions is obtained by drawing a random number from (0, 1), which is a map of the cumulative probability distribution of the number of Poisson shots. So a random number ranging from zero to a certain value represents the interval of $P(n = 0 \text{ ions})$ give the mean yield of shots. The next interval represents the range for one secondary ion etc. This gives us a number which can be interpreted as the probability in the Poisson sample space. Thus the value tells us how many secondary ions result for each shot. For these ions we draw the analogue of a flight time from Gaussian distribution with a FWHM of 5 ns (or 2.5 time bins). If two or more shots

Title Page

Abstract

Introduction

Conclusions

References

Tables

Figures

◀

▶

◀

▶

Back

Close

Full Screen / Esc

Printer-friendly Version

Interactive Discussion



occur, we determine the ions for which the dead time applies. Finally we calculate two separate line shapes. First a line with no dead time correction applied and a second one where it has been applied (Fig. 1).

From these simulations we derive some relevant statistical properties of the dead time effects. We can confirm the equations derived purely on statistical grounds by Stephan et al. (1994),

$$I_{\text{cor}} = N \ln(1 - I_{\text{exp}}/N), \quad (7)$$

where N is the number of shots in the spectrum and I_{cor} is the original count with no dead time effects and I_{exp} is the observed line with dead time effects in place. If we have a small yield, i.e. if the ratio of the number of secondary ions integrated over to shots is less than about 1/4, which corresponds to a peak value of 1/15 of the number of shots, then the intensity of the peak is reduced by the the dead time by about

$$\delta I = \left(-\frac{I}{2N} \right). \quad (8)$$

This is the case for most lines observed in COSIMA. For example if a spectrum results from 360 000 shots, and has an integrated secondary ion count of 24 000, it will loose about 800 counts or 3 % due to the dead time effects.

The dead time shifts the peak position by about

$$\Delta = -0.3 \cdot I_{\text{exp}}/N, \quad (9)$$

where Δ is in units of TOF time bins. Alternatively this can be expressed as $\Delta = -0.12 \cdot \text{FWHM} \cdot I_{\text{exp}}/N$. The shift has a statistical standard deviation of about $\sigma_{\Delta} = 1/\sqrt{N_D}$ within 10 %. For large yields and at large count values Δ has an important contribution for the position determination.

Our Bayesian approach is not affected by the two problems described above as our approach can be considered as an inverse solution by fully forward sub solutions. In



our simulation it is better that we use a model for the dead time. The magnitude of the dead time depends on the number of counts in the previous bins as the follows. A count will be recorded if there are no counts earlier in the same bin or in the previous 10 ns. This is covered by the taking into consideration half of the counts in the bin in question, and previous 5 full bins and 0.65 of the bin 5 time steps earlier. Effectively, this is calculating the conjugate of the probability of no ions in the previous bins, and thus independent of previous derivations. Using this simple formula we can model the effect of dead time effects in our simulations

$$I_{\text{dead}} = I \cdot \left(1 - \exp \left(- \frac{0.5I_0 + \sum_{i=-5}^{-1} I_i + 0.65I_{-6}}{N} \right) \right). \quad (10)$$

4.2 One weak line – analytic estimates, special case

First we make a simple example. We follow the Bayes approach, but because of the simplicity of the problem we need no simulations. We assume no background counts and a line with a total integrated number of counts as A and with internal Poisson noise only. Here we calculate the posteriori distribution, directly from a family of Poisson distributions by evaluating the likelihood of the original measured value. We give in Table 1 the median value of the distribution with confidence limits. In the case of a very low background, these values are approximately correct for a given peak. This posteriori distribution is to high degree identical to a full posteriori distribution with position and beam width parameters marginalized, with a non-informative prior, and with no dead time effects taken into account.

The differences in the mode, median and mean are important, but fortunately for our case they are not of big concern as the differences are at the most 1 count. More important for us is the asymmetry of the distributions in the case of small peaks.

If background counts are present, e.g. 10 counts in addition to a line of 20 counts, then the distribution above will be the joint distribution.



4.3 Simulated data

We calculated a set of artificial one and two peak cases to validate our method. The exact shape of the line is not critical. For simplicity we chose a Gaussian. We selected an array of 20 time bins and drew a random position for the peak randomly from $[-5, 5]$.

5 In the case of two peaks we placed them both within that interval. We drew the amplitudes randomly from a uniform distribution in $\lg(N + 1)$ space from $N = 0$ to $N = 9999$. The position of the peaks were drawn randomly from a uniform distribution between $[-10, 10]$. The FWHM was fixed to 2.5 time bins.

Before our full Bayesian tests we performed a brute force calculation. The best fit parameters were calculated at 0.1 bins in time and 20 intervals per dex in log space (resolution of a factor $10^{1/20}$ or 1.122). In total we calculated the likelihood in $(100 \times 60)^2 = 36\,000\,000$ separate data points per cases. One double peak model takes about 9.7 effective minutes to calculate on a desktop computer (ADM Athlon (tm) IIX(4) 630 Processor 2.79 GHz).

15 We calculated a total of 3300 cases with a variable background noise and different separations. The major systematic source of error is the discretization of the solutions of the data into the subbins. This is an effect that shows the weakness of the direct grid calculation of the probabilities.

A faster and more accurate estimate of the line parameters lines is obtained by the Bayesian method. The additional benefit is that we obtain a distribution of the various parameters of the solution. As an example we show an example of a real line from the COSIMA full spectrum. The example of line shown in Fig. 2 is a relatively weak line with a total number counts of about 100. The line mass is derived from the in flight measurements of constants a and b and is caused by $^{19}\text{F}^+$, which originates from the fuel of the spacecraft.

The solution for a single Gaussian gave us a mass of $19.0056\ u$ is within of $0.0077\ u$ or about 1.1 TOF time bin of $F^+ 18.9979\ u$. This is slightly more than expected. This could be explained by systematic errors or small fluctuation in the acceleration voltage.



COSIMA: Bayesian analysis

H. J. Lehto et al.

[Title Page](#)[Abstract](#)[Introduction](#)[Conclusions](#)[References](#)[Tables](#)[Figures](#)[I◀](#)[▶I](#)[◀](#)[▶](#)[Back](#)[Close](#)[Full Screen / Esc](#)[Printer-friendly Version](#)[Interactive Discussion](#)

A simulated two line case is shown in Fig. 3. The two simulated Gaussian peaks have Poisson noise added to each point. The Gaussians in this simulation have a FWHM 2.5 time flight bins or 0.031μ at mass 100μ . Both test cases have a peak with an amplitude of 1000 and a second an amplitude of 100 and total line counts of 5250 and 525.

The general peak finding algorithm detects one peak, but a two peak fit gives a better result. The x axes of Fig. 3 show the time of flight bin around mass 100, with 100μ equal to bin number 40 in these plots. In our simulation 1 time bin corresponds to 0.0125μ . The main component has tails extending over 10 time flight bins and the secondary peak is not obvious from the line shape as a primary maximum. The y axes show the total count of the line. In Fig. 3a the peaks are centered on mass 100.000 and 100.070, respectively. This corresponds to a separation of 6 bins in the peak locations. The total count is 5774. The figure shows the simulation with total counts given as a function of bins. The calculated center of lines are 100.001 and 100.076, the amplitudes are 988 and 107. The total counts are 5286 and 508, the sum of which, 5794, is very close to the original value. In Fig. 3b the peaks are centered on mass 100.000 and 100.050, respectively. This corresponds to a separation of 4 bins in the peak locations. The Bayesian solution shows lines centered on 100.001 and 100.059, the amplitudes are 1024 and 77.4. The total counts are 5521 and 397, the sum of which is 5918, close to the original value.

4.4 Bayesian case of two lines

We ran 10 000 two line simulations and modeled them with one and two peaks and investigated which of the model was correct by our Bayesian analysis. The results were quite clear cut. Two nearby peaks are not identified correctly in the presence of Bayesian noise if the following limitations are met: smaller peak has an amplitude of < 7 (or a total count of about 30), the separation is < 4.5 time bins, or the ratio of the counts of the two lines is > 1000 . These limits are for general guidance only, and need to be solved separately in each case. In our present algorithm we have a freely variable line width. With these conditions we tested a few specific interesting pairs of lines we

are able to separate ^{26}Mg from $^{12}\text{C}_2\text{H}_2$. Other nearby pairs such ^{13}C vs. ^{12}CH , ^{14}N vs. $^{12}\text{CH}_2$, ^{25}Mg vs. $^{12}\text{C}_2\text{H}$, ^{24}Mg vs. $^{12}\text{C}_2$ are not separated properly at present, agreeing with the limits from a larger set of simulations. We will investigate this in subsequent papers by fixing the position, the width or the shape of the individual spectral lines. Furthermore if the b term is larger then the resolution improves slightly rendering better results.

5 Full COSIMA spectrum

The conventional analysis of resolved time of flight mass spectrum starts with the observed spectrum, applies a correction term in order to correct for (i.e. remove) the dead time effects, and then possibly remove a background and then treat the remainder as the real line. Our analysis is nearly reverse in many aspects. We start from selecting a model from a large set of models of a beam shape, amplitude and background, after which we apply the effects of the dead time and obtain a model for an observed spectrum. Assuming a Poisson distribution for the model we then calculate the likelihood that this model explains the observations. We then iterate the solution. There are two details we should emphasize here. Our calculation is a forward calculation. For this reason we take the dead time effects into account in a reverse order than is conventional, thus we *add* the effects of the dead time to our model instead of trying to “remove” the effects from the observed data points. Note that at no point we manipulate or change the values of the real observed data. This has profound implications which we address next in more detail.

Analysis of real spectra

To analyze real COSIMA spectra we make an assumption of the line shape. We have chosen as options a Gaussian shape but on occasions a 80 % Gaussian and 20 % Lorentzian combination is an option that is suitable for modeling lines in positive spectra.

GID

4, 563–588, 2014

COSIMA: Bayesian analysis

H. J. Lehto et al.

Title Page

Abstract

Introduction

Conclusions

References

Tables

Figures

◀

▶

◀

▶

Back

Close

Full Screen / Esc

Printer-friendly Version

Interactive Discussion



If an asymmetry in the peak develops in COSIMA for any reason we will be able to take this into account. Negative ion spectra are more complicated as an additional signal before the main peak is created from by the electrons sputtered off the grids inside the reflectron. We will not discuss negative spectra in this paper in detail.

We first estimate the line amplitude and width from the observed line. To the estimated line we then apply the analytic dead time correction and obtain a model line that we can compare to the observed line. Note that here we can use the information that the probability distribution of the counts follows a Poisson distribution. With the Bayesian adaptive metropolis algorithm described earlier we can obtain the posteriori distributions of the parameters of the original line and the observed dead time effected line. These will include automatically the proper line positions and amplitudes. The total counts are obtained by summing discrete counts from the continuous model curves, so as such the fitted amplitudes of the continuous Gaussian do not represent a real quantity, but just a mathematical aid for measuring the total count from discrete abscissa values.

If we are able to give good guesses for the initial starting points for algorithm it tends to converge better to a good solution. This is not necessary for the method but aids in reducing the computing time considerably particularly in estimating multiple spectral lines simultaneously. The analysis of the lines provides a complicated challenge. Some lines are clear and isolated, often two separate lines occur. If they are sufficiently far apart, they can be treated as single isolated lines. Occasionally a section occurs in the spectrum where several lines appear to be present and mixed in. Sometimes the background levels are somewhat elevated mimicking multiple merged lines. Our approach is the following: we create a running 5 pixel boxcar sum of the spectrum of the original spectrum, find the local maximum by comparing the the adjacent smoothed pixel sums. We then accept as good guesses as points where this maximum has a value which is larger than the background. The background is defined as the smallest of two background measurements. One background estimate is obtained from the 5 pixel sum 20 pixels earlier and the second background 20 pixels of the other side of the maximum. If

GID

4, 563–588, 2014

COSIMA: Bayesian analysis

H. J. Lehto et al.

Title Page

Abstract

Introduction

Conclusions

References

Tables

Figures

◀

▶

◀

▶

Back

Close

Full Screen / Esc

Printer-friendly Version

Interactive Discussion



this difference of the boxcar of the sum and the background sum is over a certain limit we accept this point as a guess for a component. We have used an ad hoc limit of 5 counts. This is not a critical limit as it is only a first guess for our Bayesian analysis.

The Bayesian approach provides solid confidence limits for the time of flight and total counts.

6 Normalization issues, and isotope ratios

A general normalization is often performed by dividing the count of the spectral lines by a certain constant or line, e.g. Si^+ or In^+ . This is usually preceded by a removal of a variable background. This is fine for rough line identification, but possesses a problem when confidence limits are derived for the measured values. In removing and subsequent ignoring the background one obtains better looking spectra, but in this process one is introducing a poorly behaving error term on top of the noise created by the “Poisson noise”. Poisson noise is additive but not subtractive. Furthermore, in calculating the ratios of lines the determination of the confidence limits becomes formally ill behaved, as the divider, the reference line has in principle a probability distribution which includes zero. These are serious issues when any one of the lines is a weak one. If the lines in question are strong, and in particular the reference line is a strong one, say at least a thousand counts, then the the distortion may not be serious, if the background counts are at the same time low, say less than 50.

The proper way to normalize is to build a model where the line ratio is solved for. Take a guess of the stronger integrated line count, make a good guess of the background, and apply an isotope ratio. You have now calculated two integrated line counts. Using the Poisson distribution calculate what is the likelihood that the observe lines are explained by the given model. Continue with the Bayesian principles of searching for the posteriori probability distribution. Finally marginalize (integrate) over background and amplitudes to get the likelihood of the isotope distribution.

Title Page

Abstract

Introduction

Conclusions

References

Tables

Figures

◀

▶

◀

▶

Back

Close

Full Screen / Esc

Printer-friendly Version

Interactive Discussion



7 Line identifications of specific lines

The spectra are provided with an initial estimate of the scaling parameters, a and b . We have built a simple line identification scheme with the elemental lines and a small set of simple organic lines. These can be applied to the observed values and further improvement with a larger set of lines is possible removing systematic trends evident in the original spectra as shown in Figs. 2 or 4.

In this study we have considered so far all lines as independent in the sense that the background level, the line width, position and the maximum amplitude of the peak have been free parameters. However, if we wish to ask a specific question such as does certain mass contain lines at predefined exact masses, we can employ different variations to the analysis. For example, if we see separately ^{24}Mg and $^{12}\text{C}_2$, we may want to ask whether mass 25 contains $^{25}\text{Mg}^+$, $^{24}\text{MgH}^+$ and $^{12}\text{C}_2\text{H}^+$. We can then fix the interval of the lines in mass and solve for the background level, a single mass offset, and the amplitudes (and the widths) of the three peaks. This reduces the adjustable parameter space from 10 to 8 or 5.

An additional set up can be created between the above multiline kind example and isotope ratios. Consider e.g. the lines $^{12}\text{C}^+$, $^{13}\text{C}^+$, $^{12}\text{CH}^+$. We can use a model where the ratio of $^{13}\text{C}^+ / ^{12}\text{C}^+$ has a cosmic value, so that is not a free parameter. Two free parameters are the position and the amplitude of $^{12}\text{C}^+$. One free parameter is the position and amplitude of $^{12}\text{CH}^+$. The isotope ratio fixes the amplitude of $^{13}\text{CH}^+$, and the mass is fixed by mass difference the mass, so unless we consider the width of the line being an additional free parameter, it will have really no free parameters, and this whole model will have 5 (or 8) free parameters.

Investigating the full parameter space of all possible models is beyond the scope of this paper, but we wish to point out the generality of the Bayesian method. These kind of analyses are not easy to do with conventional means, and the posteriori probability distributions are then only guesses. We thus provide posteriori distributions and confidence limits for the measured parameters.

GID

4, 563–588, 2014

**COSIMA: Bayesian
analysis**

H. J. Lehto et al.

Title Page

Abstract

Introduction

Conclusions

References

Tables

Figures

◀

▶

◀

▶

Back

Close

Full Screen / Esc

Printer-friendly Version

Interactive Discussion



8 Conclusions

We have discussed the basic principles of applying a Bayesian approach to the analysis of COSIMA spectra. We address its accuracy, the fundamental principles and discuss the possibilities that analysis method has.

The instrumental properties of COSIMA that simplify our analysis are the long time interval between the shots so that the secondary ions formation and flight time of the ions can be considered usually statistically independent from shot to shot. Second, the shortness of the pulse and the well calibrated instrument means that not only each mass line but often the organic and mineral components can be analyzed separately. Third, the dead time is relatively short and quite nicely matched with the line width, so the dead time effects will not leak to neighboring lines. The narrow line shape means that the spectra cannot be well modeled by a line shape derived from the spectrum.

Acknowledgements. COSIMA was built by a consortium led by the Max-Planck-Institut für Extraterrestrische Physik, Garching, Germany in collaboration with Laboratoire de Physique et Chimie de l'Environnement, Orléans, France, Institut d'Astrophysique Spatiale, CNRS/INSU and Université Paris Sud, Orsay, France, Finnish Meteorological Institute, Helsinki, Finland, Universitaät Wuppertal, Wuppertal, Germany, von Hoerner und Sulger GmbH, Schwetzingen, Germany, Universität der Bundeswehr, Neubiberg, Germany, Institut für Physik, Forschungszentrum Seibersdorf, Seibersdorf, Austria, Institut für Weltraumforschung, Österreichische Akademie der Wissenschaften, Graz, Austria and is lead by the Max-Planck-Institut für Sonnensystemforschung, Göttingen, Germany. The support of the national funding agencies of Germany (DLR), France (CNES), Austria and Finland and the ESA Technical Directorate is gratefully acknowledged. We thank the Rosetta Science Ground Segment at ESAC, the Rosetta Mission Operations Centre at ESOC and the Rosetta Project at ESTEC for their outstanding work enabling the science return of the Rosetta Mission.

GID

4, 563–588, 2014

COSIMA: Bayesian analysis

H. J. Lehto et al.

Title Page

Abstract

Introduction

Conclusions

References

Tables

Figures

◀

▶

◀

▶

Back

Close

Full Screen / Esc

Printer-friendly Version

Interactive Discussion



References

Batir, N.: Very Accurate approximation for the factorial function, *J. Math. Inequal.*, 4, 335–344, 2010.

Gelman, A., Carlin, J. B., Stern, H. S., and Rubin, D. B.: *Bayesian Data Analysis*, Chapman & Hall, London, 1995. 571

Glassmeier, K. H., Boehnhardt, H., Koschny, D., Kührt, E., and Richter, I.: The Rosetta mission: flying towards the origin of the Solar System, *Space Sci. Rev.*, 128, 1–21, 2007. 564

Haario, H., Saksman, E., and Tamminen, J.: An adaptive Metropolis algorithm, *Bernoulli*, 7, 223–242, 2001. 572

Kissel, J., Altwegg, K., Clark, B. C., Colangeli, L., Cottin, H., Czempiel, S., Eibl, J., Engrand, C., Fehrer, H. M., Feuerbacher, B., Fomenkova, M., Glasmachers, A., Greenberg, J. M., Grün, E., Haerendel, G., Henkel, H., Hilchenbach, M., von Hoerner, H., Höfner, H., Hornung, K., Jessberger, E. K., Koch, A., Krüger, H., Langevin, Y., Parigger, P., Raulin, F., Rüdener, F., Rynö, J., Schmid, E. R., Schulz, R., Silén, J., Steiger, W., Stephan, T., Thirkell, L., Thomas, R., Torkar, K., Utterback, N. G., Varmuza, K., Wanczek, K. P., Werther, W., and Zscheeg, H.: COSIMA – high resolution time-of-flight secondary ion mass spectrometer for the analysis of cometary dust particles onboard Rosetta, *Space Sci. Rev.*, 128, 823–867, 2007. 565, 566, 567

Silén, J., Cottin, H., Hilchenbach, M., Kissel, J., Lehto, H., Siljeström, S., and Varmuza, K.: COSIMA data analysis using multivariate techniques, *Geosci. Instrum. Method. Data Syst. Discuss.*, 4, 455–489, doi:10.5194/gid-4-455-2014, 2014. 565

Stephan, T., Zehnpfening, J., and Benninghoven, A.: Correction of dead time effects in time-of-flight mass spectroscopy, *J. Vac. Sci. Technol. A*, 12, 405–410, 1994. 574

Tamminen, J.: *Adaptive Markov Chain Monte Carlo Algorithms with Geophysical Applications*, Finnish Meteorological Institute Contributions No. 47, Ph.D. Thesis, University of Helsinki, Dept. of Mathematics and Statistics, Helsinki, 2004. 573

GID

4, 563–588, 2014

COSIMA: Bayesian analysis

H. J. Lehto et al.

Title Page

Abstract

Introduction

Conclusions

References

Tables

Figures

◀

▶

◀

▶

Back

Close

Full Screen / Esc

Printer-friendly Version

Interactive Discussion



COSIMA: Bayesian analysis

H. J. Lehto et al.

[Title Page](#)[Abstract](#)[Introduction](#)[Conclusions](#)[References](#)[Tables](#)[Figures](#)[I◀](#)[▶I](#)[◀](#)[▶](#)[Back](#)[Close](#)[Full Screen / Esc](#)[Printer-friendly Version](#)[Interactive Discussion](#)**Table 1.** Posteriori distributions of a Poisson peak with a given amplitude A_{obs} , and no background noise.

A_{obs}	2	3	5	7	10	15	20	30
$A_{\text{low } 99}$	0.1	0.6	1.5	2.5	4.3	7.5	11.0	18.5
$A_{\text{low } 90}$	0.3	1.3	2.6	3.9	6.1	10.0	14.1	22.4
$A_{\text{low } 68}$	1.7	2.0	3.6	5.2	7.7	12.0	16.4	24.4
$A_{\text{low } 50}$	1.7	2.6	4.2	5.8	8.6	13.1	17.7	27.0
A_{mode}	2.0	3.0	5.0	7.0	10.0	15.0	20.0	30.0
A_{median}	2.5	3.5	5.5	7.5	10.5	15.5	20.5	30.5
$\langle A \rangle$	3.0	4.0	6.0	8.0	11.0	16.0	21.0	31.0
$A_{\text{high } 50}$	3.8	5.1	7.4	9.6	13.0	18.4	23.8	34.5
$A_{\text{high } 68}$	4.6	5.9	8.3	10.7	14.2	19.9	25.5	36.5
$A_{\text{high } 90}$	5.3	7.7	10.5	13.1	16.9	23.0	29.0	40.6
$A_{\text{high } 99}$	12.0	10.9	14.0	17.1	21.3	28.1	34.6	47.2
$\sqrt{A_{\text{obs}}}$	1.4	1.7	2.2	2.7	3.2	3.9	4.5	5.5

We should note that although the single highest probability A_{mode} is the same as the observed value, the median value has a bias of +0.5 and the mean of the distribution has an even larger positive bias of 1.0. The total width of the 68 % confidence limits agree within roundoff errors with \sqrt{A} the median point is not centered on the limits. Other low and high confidence limits are shown. Note that as they are asymmetric both lower and higher limits are shown for the important confidence limits. The distributions are clearly asymmetric with a positive skew.

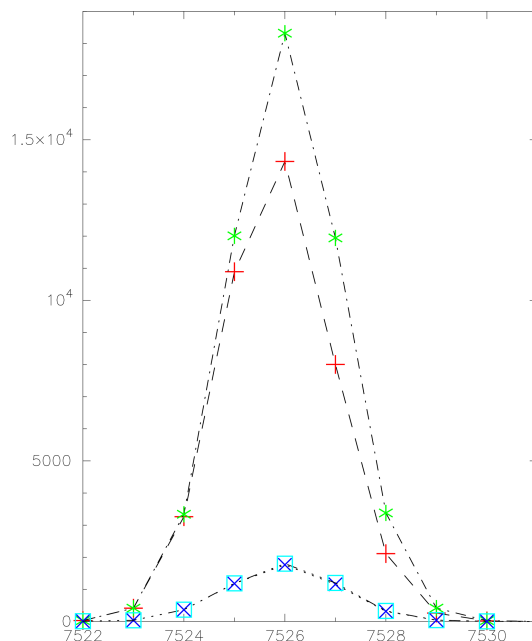


Figure 1. Effects of dead time in COSIMA. The effect is shown on for two artificial Gaussian lines. The strongest line has a total yield of 50 %. The fainter line has a yield of 5 %. The top most curve (green stars and dot dash line) shows the original 50 % curve, the second curve (red crosses, dash line) show how the dead time effect has changed the curve. This is in principle the observed line. Note how the maximum and correspondingly the total line count has decreased. Also note how the line center and peak has shifted to the left. This is particularly noteworthy on the right side of the line. The lower two curves show similar cases for the 5 % line with blue squares, purple crosses, respectively.

Title Page

Abstract

Introduction

Conclusions

References

Tables

Figures

I◀

▶I

◀

▶

Back

Close

Full Screen / Esc

Printer-friendly Version

Interactive Discussion



COSIMA: Bayesian analysis

H. J. Lehto et al.

Title Page

Abstract

Introduction

Conclusions

References

Tables

Figures

◀

▶

◀

▶

Back

Close

Full Screen / Esc

Printer-friendly Version

Interactive Discussion

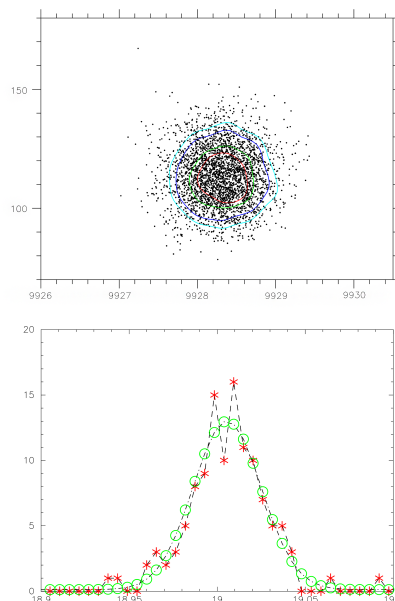


Figure 2. An example of the posteriori distribution of a weak line at mass 19. The background around the line is very low, the weak line has an observed maximum of 16 counts. The top panel shows the posteriori distributions in total count vs. time flight bin. The red curve contains 50 % posteriori confidence limits, green curve 68 %, dark blue 90 % and the light blue 95 % limits. Note that the most likely value has a rather symmetric distribution with 68 % confidence width of about 0.34 TOF time bins or $0.002\,u$ in mass, and integrated mean count of 113 ± 11 counts. The mass $19.0056\,u$ is within $0.0077\,u$ or $F^+ 18.9979\,u$. The line does not agree quite as well with heavy water HDO^+ of mass $19.0162\,u$ nor the hydrogenated water ion (hydronium) H_3O^+ with a mass of $19.0178\,u$. These are off by which by 0.0106 and $0.0122\,u$ respectively from the calculated line position. The expected hydronium line would have a time of flight bin of 9929.53, not in agreement with the posteriori distribution of the upper panel. The spectrum used here is from the flight model CS_2D8_20100509T194035_SP_P.TAB.

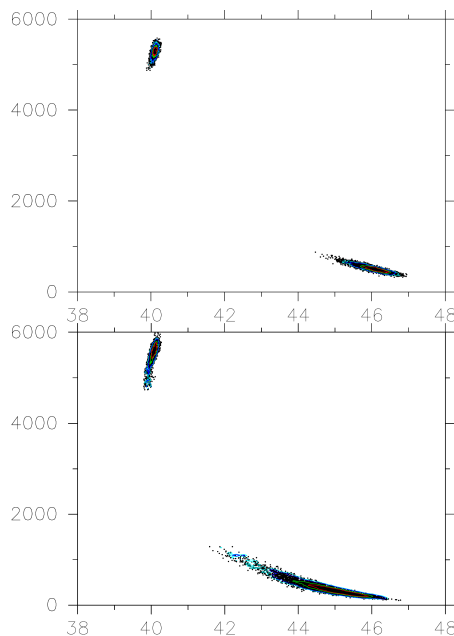


Figure 3. Two examples of the posteriori distributions of the amplitudes and positions. The two simulated Gaussian peaks have Poisson noise added to each point. The Gaussians have a FWHM 2.5 time flight bins or $0.031\,u$ at mass $100\,u$. Both test cases have a peak with an amplitude of 1000 and a second an amplitude of 100 with total bin counts of 5250 and 525, respectively. In the first case the peaks are located are separated by 6 bins and in the second simulation by 6 bins. The red curve contains 50 % posteriori confidence limits, green curve 68 %, dark blue 90 % and the light blue 95 % limits. Note that the distribution maxima are well defined and close to the initial values. Note that the distributions have a low density tails which reflect the fact that there is mild degeneracy in the solution.

COSIMA: Bayesian analysis

H. J. Lehto et al.

Title Page

Abstract

Introduction

Conclusions

References

Tables

Figures

I◀

▶I

◀

▶

Back

Close

Full Screen / Esc

Printer-friendly Version

Interactive Discussion

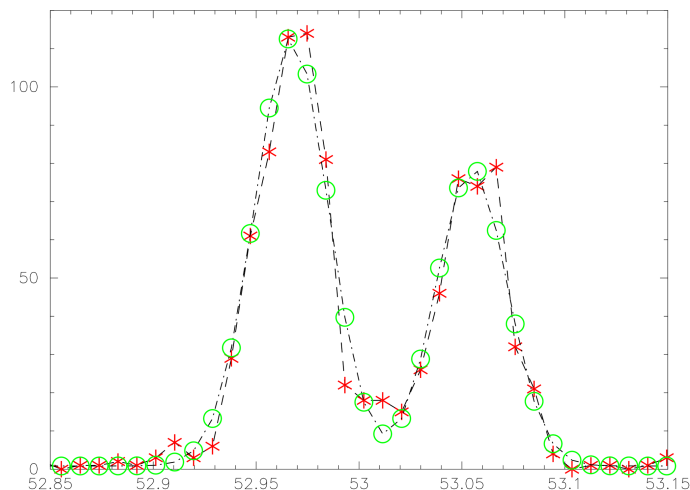


Figure 4. An example of the the mass 53 spectral lines in a RM spectrum CS_45D_20110309T074148_SP_P.TAB. The model fit here is a two Gaussian model and a constant background. The observed line is shown with the red stars and the fit with green circles. The masses derived are 52.967 and 53.055 u . The masses suggest a systematic error of +0.022 u in mass and an identification of $^{53}\text{Cr}^+$ at 52.9401 u and C_4H_5^+ at mass 53.0386 u .